

COMMUNICATION

CrossMark
click for updatesCite this: *Nanoscale*, 2014, 6, 11062Received 5th July 2014
Accepted 31st July 2014

DOI: 10.1039/c4nr03754e

www.rsc.org/nanoscale

Adsorption-geometry induced transformation of self-assembled nanostructures of an aldehyde molecule on Cu(110)[†]Chi Zhang,[‡] Qiang Sun,[‡] Kai Sheng, Qinggang Tan and Wei Xu^{*}

From an interplay of high-resolution STM imaging/manipulation and DFT calculations, we have revealed that different self-assembled nanostructures of BA molecules on Cu(110) are attributable to specific molecular adsorption geometries, and thus the corresponding intermolecular hydrogen bonding patterns. The STM manipulations demonstrate the feasibility of switching such weak-hydrogen-bonding patterns.

Supramolecular architectures from molecular self-assembly on solid surfaces have received significant attention due to the attached new functionalities and a multitude of potential applications in biochemical sensors, chiral catalysis, and organic electronics.^{1–3} One prerequisite to achieve well-defined nanostructures is an exhaustive exploration of the influencing factors dominating the entire self-assembly processes. For intrinsic factors, different kinds of intermolecular interactions typically involving functional groups such as nitrile,^{4–6} amine^{7,8} and carboxyl group^{9,10} have been extensively explored, and well-ordered nanostructures have been achieved. Further, external stimuli, such as STM manipulations^{11–13} and UV irradiation,¹⁴ have proved to be effective for influencing the self-assembled nanostructures. However, to our knowledge, on-surface self-assembly of an aldehyde molecule has been rarely reported,^{15,16} and in-depth exploration and controllable switching of intermolecular interactions in relation to molecular adsorption geometries have not been particularly emphasized upon in previous studies. Understanding the details of molecular self-assembly and forced-assembly processes may shed light on designing man-made molecular nanostructures.

In this work, we have explored the self-assembly of an aromatic aldehyde molecule (biphenyl-4-carboxaldehyde (shortened as BA)) on a Cu(110) substrate under ultrahigh

vacuum (UHV) conditions. From an interplay of high-resolution scanning tunneling microscopy (STM) imaging/manipulation and density functional theory (DFT) calculations, we have investigated the self-assembly of BA molecules at various coverages where different intermolecular hydrogen bonding patterns in relation to molecular adsorption geometries are explored in depth. At low coverage, we found that the BA molecules prefer to adsorb on the surface in two specific directions (*i.e.* $\pm 35^\circ$ with respect to the [001] direction of the substrate) and form discrete clusters typically as windmill-like tetramers bound by weak intermolecular hydrogen bonds. At high coverage (~ 1 ML), we found the formation of well-ordered close-packed molecular nanostructures, and interestingly, inside the structures, some specific BA molecules exhibited one additional adsorption direction (*i.e.* along the [001] direction) resulting from molecular packing and different hydrogen bonding patterns. By *in situ* STM manipulations, we surprisingly found that the hydrogen bonding pattern appearing in the high-coverage structure could be artificially achieved in the low-coverage one. These results demonstrate the versatility of weak hydrogen bonding in the fabrication of on-surface molecular nanostructures and the capability of STM manipulation technique in switching intermolecular hydrogen bonding patterns, which may be extended into more complicated systems with the aim of designing functional nanostructures *via* the bottom-up strategy.

The STM experiments were performed in a UHV chamber (base pressure: 1×10^{-10} mbar) equipped with a variable-temperature “Aarhus-type” STM purchased from SPECS,^{17,18} a molecular evaporator and standard facilities for sample preparation. After the system was thoroughly degassed, the molecules were deposited by thermal sublimation onto a Cu(110) substrate. The sample was, thereafter, transferred within the UHV chamber to the STM, where measurements were carried out at ~ 100 K. The lateral manipulations were carried out in a controllable line-scan mode under specific scanning conditions (by increasing the tunnel current up to approximately 2.0 nA while reducing the tunnel voltage down to approximately 20

College of Materials Science and Engineering, Tongji University, Caoan Road 4800, Shanghai 201804, P. R. China. E-mail: xuwei@tongji.edu.cn

[†] Electronic supplementary information (ESI) available: Supplementary STM images and DFT calculation results. See DOI: 10.1039/c4nr03754e

[‡] These authors contributed equally.

mV^{19,20}). All the calculations were carried out in the framework of DFT by using the Vienna *ab initio* simulation package (VASP).^{21,22} The projector augmented wave method was used to describe the interaction between ions and electrons.^{23,24} We employed the PBE-GGA as the exchange–correlation functional²⁵ and van der Waals interactions were included using the DFT-D2 method of Grimme.²⁶ The atomic structures were relaxed using the conjugate gradient algorithm scheme as implemented in the VASP code until the forces on all the unconstrained atoms were ≤ 0.03 eV \AA^{-1} .

After the deposition of BA molecules on the Cu(110) substrate held at RT, we found that the molecules can form discrete clusters in which two specific molecular adsorption directions are identified (*cf.* Fig. 1a), and these clusters are mainly constituted by two kinds of chiral windmill-like tetramers as building blocks, as revealed by the high-resolution STM images (*cf.* Fig. 1b). According to the STM observations, we have carried out systematic structural search by proposing different possible tetramers and finally obtained the energetically most favorable structural models including the substrate, as shown in Fig. 1c and e, which are also superimposed on top of the corresponding close-up STM images, respectively, and good agreements are achieved (*cf.* Fig. 1b). As depicted in Fig. 1c and e, we can identify that within the tetramer structures, the BA molecules interact with each other *via* different weak C–H \cdots O hydrogen bonds as indicated by the blue dotted lines, and the charge density difference maps plotted in Fig. 1d and f help to further recognize the hydrogen bonding patterns in the tetramer structures.

To further investigate the self-assembly of BA molecules at higher coverages and the interactions among the neighboring BA molecules, we have varied the coverages up to ~ 1 ML (for the coverages at ~ 0.7 – 1.0 ML, see Fig. S1[†]). Interestingly, after the deposition of BA molecules at ~ 1 ML coverage on Cu(110) held at RT with subsequent annealing to 370 K, we observe the formation of well-ordered close-packed nanostructures with only two growing directions, as shown in Fig. 2a. As illustrated in the close-up STM image (*cf.* Fig. 2b), besides the original molecular adsorption directions (*i.e.* 35° with respect to the [001] direction indicated by the blue arrow, which is consistent with that within the discrete clusters formed at low coverage), one additional adsorption direction of the BA molecule (*i.e.* along the [001] direction indicated by the green arrow) is observed. The slight difference in the apparent topography of the BA molecules along the [001] direction within the close-packed nanostructures may be due to the different tip states as in some cases, there is no difference (*cf.* Fig. S2[†]). It appears that the molecules with two original adsorption orientations preferentially arrange in a side-by-side mode to form ordered stripes, typically ranging from two to four columns (more columns exist as well) (*cf.* Fig. S3 and S4[†]) that are always alternately separated by single-column molecules with the molecular adsorption direction along the [001] direction. Interestingly, as illustrated by the line-scan profiles (*cf.* Fig. 2c), we can identify that the left and right neighboring molecules of the single-column molecules adopt an anti-parallel arrangement. Based on the STM indications discussed above, different

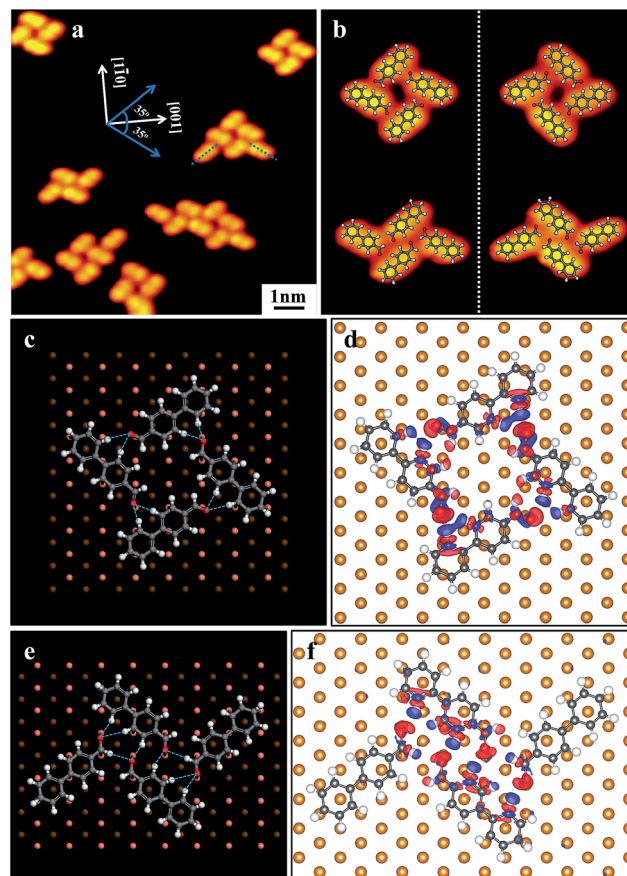


Fig. 1 (a) STM image showing the formation of discrete clusters after the deposition of BA molecules at low coverage (~ 0.1 ML) on the Cu(110) substrate held at room temperature (RT). The blue arrows (parallel to the dashed lines) indicate the two adsorption directions of BA molecules (*i.e.* $\pm 35^\circ$ with respect to the [001] direction). (b) The high-resolution STM images of the typical tetramers with the DFT optimized structural models superimposed. The corresponding enantiomers are separated by a white dotted line. Scanning conditions: $I_t = 1.38$ nA, $V_t = -1250$ mV. (c) and (e) show the DFT optimized structural models of the two kinds of tetramers including the Cu(110) substrate and the corresponding charge density difference maps (the four molecules on the substrate are considered to be four individual species and the charge transfers between four individual molecules and the substrate have been subtracted) are shown in (d) and (f), respectively. The hydrogen bonds are indicated by blue dotted lines in (c) and (e). The isosurface values in (d) and (f) are at the same level of 0.0007 e \AA^{-3} . Blue and red isosurfaces indicate charge depletion and accumulation, respectively. O: red, C: gray, H: white, first layer Cu atoms: bronze, second layer Cu atoms: brown. Cu atoms in (d) and (f) golden.

gas-phase structural models (with the molecular columns typically ranging from two to four) have been optimized and the energetically most favorable ones have been shown in Fig. S3[†] and good agreements are achieved. Furthermore, we have carried out systematic research on the simplified structure composed of two molecular columns and one separating single-column as the unit cell and we finally obtain the energetically most favorable structural model of the close-packed nanostructure including the substrate, as shown in Fig. 2d. From the optimized model, we can identify that the molecules within the

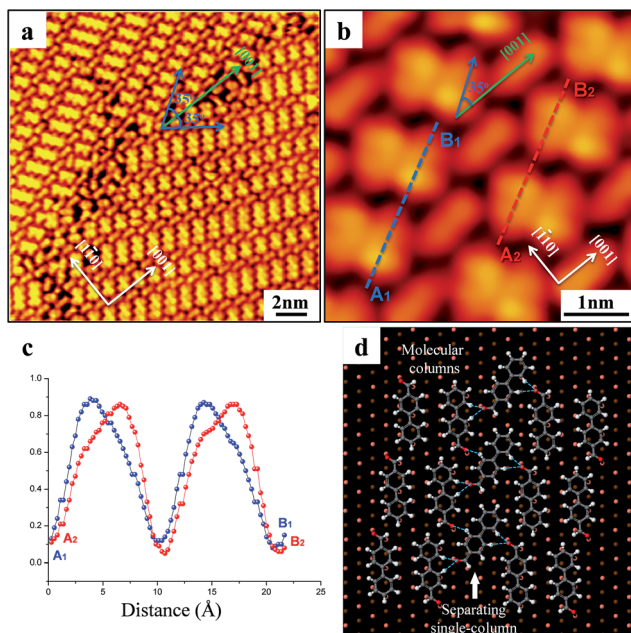


Fig. 2 (a) Large-scale STM image showing the formation of a close-packed nanostructure after the deposition of BA molecules at high coverage (~ 1 ML) on the Cu(110) substrate held at RT and subsequent annealing to ~ 370 K for 10 min. The blue arrows and green arrow indicate the two original molecular adsorption directions (*i.e.* $\pm 35^\circ$ with respect to the [001] direction) and the one additional adsorption direction (*i.e.* along the [001] direction), respectively. (b) The close-up STM image of the close-packed nanostructure. Scanning conditions: $I_t = 1.24$ nA, $V_t = -2100$ mV. (c) The line-scan profiles along the blue and red dotted lines illustrated in (b). (d) The DFT optimized structural model of the typical close-packed nanostructure including the Cu(110) substrate.

single column interact with the neighboring molecules by a new C–H \cdots O hydrogen bonding pattern. Thus, the main driving forces for the formation and stabilization of the close-packed nanostructures are molecular packing and squeezing (to induce a different molecular adsorption direction, that is, along the [001] direction) at high coverages and then forming the weak hydrogen bonds between the single-column molecules and the neighboring molecules at the two sides. The anti-parallel arrangement of the neighboring molecules beside the single molecular column results only from such intermolecular interaction. The intermolecular forces within the side-by-side molecular columns are mainly van der Waals (vdW) interactions.

To unravel the nature of the differences between the two self-assembled nanostructures (*i.e.* discrete clusters and close-packed structures) and explore the possibility of switching different hydrogen bonding patterns, we have performed a series of delicate *in situ* STM manipulations, as shown in Fig. 3. After the manipulation of the cluster structure formed at low molecular coverage (*cf.* Fig. 3a and b), two molecules could be detached from the cluster indicating a relatively weak C–H \cdots O intermolecular hydrogen bonding characteristic. Further manipulation on the remaining cluster (*cf.* Fig. 3b) results in the switching of the molecular adsorption geometries of molecules A and B (as marked in Fig. 3b) (*cf.* Fig. 3c), that is, molecule A is

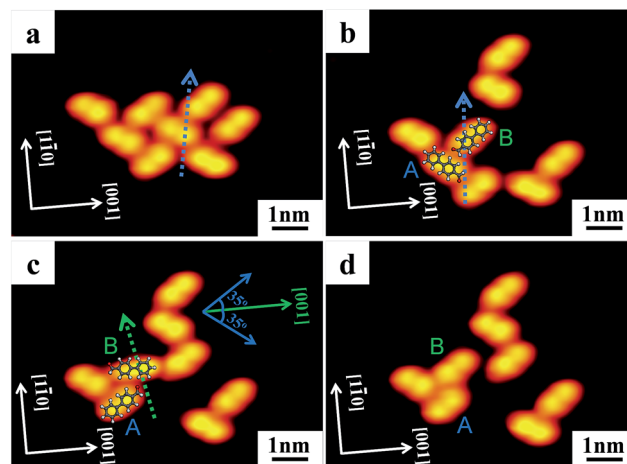


Fig. 3 Lateral STM manipulations of the cluster structures formed at low molecular coverage (~ 0.1 ML). The blue and green arrows in (a–c) indicate the directions of STM manipulation. Manipulation conditions: $I_t = 2$ nA, $V_t = 20$ mV. Scanning conditions: $I_t = 1.33$ nA, $V_t = -1250$ mV.

switched to its symmetric direction with respect to the [001] direction (*i.e.* $\pm 35^\circ$ with respect to the [001] direction as discussed above), and interestingly, molecule B is switched to the [001] direction, which is only observed in the high-coverage nanostructures. A closer inspection of the high-resolution STM images together with the superimposed molecular models (which correspond to the structural models shown in Fig. 1c and 2d) (*cf.* Fig. 3b and c) reveals that such STM manipulation actually results in the switching of different hydrogen bonding patterns from the one formed in the tetramer structure at low coverage (*cf.* Fig. 1c) to the one formed in the close-packed structure at high coverage (*cf.* Fig. 2d). Further, the adsorption geometry of molecule B can be switched back to the original one (*cf.* Fig. 3c and d).

In conclusion, from an interplay of high-resolution STM imaging/manipulation and DFT calculations, we have revealed that different self-assembled nanostructures of BA molecule on Cu(110) are attributable to specific molecular adsorption geometries, and thus, the corresponding intermolecular hydrogen bonding patterns, and lateral STM manipulations demonstrate the feasibility of switching such weak-hydrogen-bonding patterns. The results would supplement the understanding of on-surface supramolecular self-assembly processes through weak intermolecular interactions and may also shed light on the rational design of artificial supramolecular architectures on solid surfaces.

Acknowledgements

The authors acknowledge the financial supports from the National Natural Science Foundation of China (21103128), the Shanghai “Shu Guang” Project supported by Shanghai Municipal Education Commission and Shanghai Education Development Foundation (11SG25), the Fundamental Research Funds for the Central Universities, the Research Fund for the Doctoral Program of Higher Education of China (20120072110045).

Notes and references

- 1 Y. Ke, S. Lindsay, Y. Chang, Y. Liu and H. Yan, *Science*, 2008, **319**, 180.
- 2 C. J. Baddeley, *Top. Catal.*, 2003, **25**, 17.
- 3 S. Lei, J. Puigmarti-Luis, A. Minoia, M. Van der Auweraer, C. Rovira, R. Lazzaroni, D. B. Amabilino and S. De Feyter, *Chem. Commun.*, 2008, 703.
- 4 T. Yokoyama, S. Yokoyama, T. Kamikado, Y. Okuno and S. Mashiko, *Nature*, 2001, **413**, 619.
- 5 U. Schlickum, R. Decker, F. Klappenberger, G. Zoppellaro, S. Klyatskaya, M. Ruben, I. Silanes, A. Arnau, K. Kern, H. Bruneand and J. V. Barth, *Nano Lett.*, 2007, **7**, 3813.
- 6 U. Schlickum, R. Decker, F. Klappenberger, G. Zoppellaro, S. Klyatskaya, W. Auwarter, S. Nepl, K. Kern, H. Brune, M. Rubenand and J. V. Barth, *J. Am. Chem. Soc.*, 2008, **130**, 11778.
- 7 R. E. A. Kelly, W. Xu, M. Lukas, R. Otero, M. Mura, Y. J. Lee, E. Lægsgaard, I. Stensgaard, L. N. Kantorovich and F. Besenbacher, *Small*, 2008, **4**, 1494.
- 8 H. Kong, Q. Sun, L. Wang, Q. Tan, C. Zhang, K. Sheng and W. Xu, *ACS Nano*, 2014, **8**, 1804.
- 9 S. Karan, Y. Wang, R. Robles, N. Lorente and R. Berndt, *J. Am. Chem. Soc.*, 2013, **135**, 14004.
- 10 S. De Feyter and F. C. De Schryver, *Chem. Soc. Rev.*, 2003, **32**, 139.
- 11 W. Xu, H. Kong, C. Zhang, Q. Sun, H. Gersen, L. Dong, Q. Tan, E. Laegsgaard and F. Besenbacher, *Angew. Chem., Int. Ed.*, 2013, **52**, 7442.
- 12 W. Xu, C. Zhang, H. Gersen, Q. Sun, H. Kong, L. Dong, K. Sheng, Q. Tan, E. Lægsgaard and F. Besenbacher, *Chem. Commun.*, 2013, **49**, 5207.
- 13 S. Selvanathan, M. V. Peters, S. Hecht and L. Grill, *J. Phys.: Condens. Matter*, 2012, **24**, 354013.
- 14 D. Wang, Q. Chen and L. J. Wan, *Phys. Chem. Chem. Phys.*, 2008, **10**, 6467.
- 15 S. Weigelt, C. Busse, C. Bombis, M. M. Knudsen, K. V. Gothel, T. Strunskus, C. Wöll, M. Dahlbom, B. Hammer, E. Lægsgaard, F. Besenbacher and T. R. Linderoth, *Angew. Chem., Int. Ed.*, 2007, **119**, 9387.
- 16 S. Weigelt, C. Bombis, C. Busse, M. M. Knudsen, K. V. Gothelf, E. Lægsgaard, F. Besenbacher and T. R. Linderoth, *ACS Nano*, 2008, **2**, 651.
- 17 F. Besenbacher, *Rep. Prog. Phys.*, 1996, **59**, 1737.
- 18 E. Lægsgaard, L. Österlund, P. Thostrup, P. B. Rasmussen, I. Stensgaard and F. Besenbacher, *Rev. Sci. Instrum.*, 2001, **72**, 3537.
- 19 M. Yu, W. Xu, Y. Benjalal, R. Barattin, E. Laegsgaard, I. Stensgaard, M. Hliwa, X. Bouju, A. Gourdon, C. Joachim, T. R. Linderoth and F. Besenbacher, *Nano Res.*, 2009, **2**, 254.
- 20 F. Rosei, M. Schunack, P. Jiang, A. Gourdon, E. Laegsgaard, I. Stensgaard, C. Joachim and F. Besenbacher, *Science*, 2002, **296**, 328.
- 21 G. Kresse and J. Hafner, *Phys. Rev. B: Condens. Matter Mater. Phys.*, 1993, **48**, 13115.
- 22 G. Kresse and J. Furthmüller, *Phys. Rev. B: Condens. Matter Mater. Phys.*, 1996, **54**, 11169.
- 23 P. E. Blöchl, *Phys. Rev. B: Condens. Matter Mater. Phys.*, 1994, **50**, 17953.
- 24 G. Kresse and D. Joubert, *Phys. Rev. B: Condens. Matter Mater. Phys.*, 1999, **59**, 1758.
- 25 J. P. Perdew, K. Burke and M. Ernzerhof, *Phys. Rev. Lett.*, 1996, **77**, 3865.
- 26 S. Grimme, *J. Comput. Chem.*, 2006, **27**, 1787.